YBCO-on-Kapton: Material for High-Density Quantum Computer Interconnects with Ultra-Low Thermal Conductance

Vyacheslav Solovyov, Olli-Pentti Saira, Zachary Mendleson, and Ilya Drozdov

***Abstract*— Development of practical quantum computers would require 1000's of qubits and equally large number of read-outs, bias and drive lines. New materials that combine low passive loss and good RF properties are needed. Here we report performance of signal interconnects comprised of high-temperature YBCO films that are exfoliated from a metal substrate and transferred to a E-Kapton tape. The technology offers low-loss transition between 60 K to sub-mK environments and interfacing with off-shelf flexible silicon electronics. We demonstrate < 1 dB/m attenuation at 6 GHz at 77 K. The microstrip assemblies demonstrated no degradation upon multiple cycles to liquid Nitrogen and conduction cooling down to 18 K. We discuss designs of a practical high-density signal cable with passive heat load well below 1 μW per line. The YBCO-on-Kapton technology offers a practical pathway to large error-corrected quantum computing systems.**

***Index Terms*— High-temperature superconductors, quantum computing, RF properties, thermal conductivity**

I. Introduction

IT is recognized that a practical, error-corrected quantum computer would incorporate 1000's of qubits. Each qubit would need separate drive, read-out and flux-bias lines; additionally, gate lines might be desirable to introduce inter-qubit coupling. An optimized Wiedemann-Franz metal conductor delivers approximately 90 mW of heat per 1 A into > 4 K stage when operating in DC mode [1]. At frequencies > 1 GHz, skin effect losses become significant and impose an attenuation constant (in dB/m) of $8.68*R_0/(2*Z_0)$, where R_0 is the series resistance per length, and Z_0 is the characteristic impedance. In a large system, the combined heat load of 1,000's of signal and bias lines would easily exceed the cooling power of a standard dilution refrigerator. For example, a 50 qubit processor with 150 RF lines cooled by a Bluefors XLD400 DR dilution refrigerator would operate at 20% capacity on 50 K stage and 30% capacity at the mixing chamber flange [2]. Scaling such a design to 1,000's of qubits would require several standard cryocoolers and dilution units, resulting in a bulky and expensive setup.

Superconducting signal lines allow circumventing the limitation of a Wiedemann-Franz metal, at least at temperature below T_c. Coaxial lines [3] and flexible cables [4, 5] based on Nb-Ti alloy have been successfully implemented in quantum computes and quantum detector systems. Compact strip-lines were manufactured by depositing Nb metal on Kapton [6].

The Nb-based lines operate below 10 K, still necessitating use of traditional metal cables between room temperature and 4 K. High-temperature superconductors (HTS) offer direct superconducting connection between 77 - 50 K stage and sub-kelvin environment. Because off-shelf Si electronics work well down to 50 K, an efficient and compact interface can be designed by placing signal conditioning and multiplexing on the 50 K flange. It is well known that HTS compounds exhibit good RF properties only in a form of a bi-axially aligned film or a single crystal. A bi-axially aligned HTS film can only be synthesized by a high-temperature (> 700°C) epitaxial growth on a lattice-matched ceramic substrate. So-called second-generation (2G) conductor process [7] uses flexible metal substrates coated with ceramic layers to grow high-quality $YBa_2Cu_3O_7$ (YBCO) epitaxial films on kilometer scale. In a traditional 2G tape application, the substrate is an integral part of the conductor architecture and is incorporated into a superconducting device. A superconductor on a metal substrate can be tolerated in a magnet winding but is obviously unsuitable in a RF device, where the metal would introduce significant RF loss.

Recently we developed a process for exfoliation of YBCO layer from the supporting metal substrate [8]. The epitaxial YBCO film, typically 1 μm thick, can now be transferred onto a metal or dielectric support material. In this work we demonstrate how polyimide (DuPont Kapton) can be used as the support for epitaxial YBCO films exfoliated from commercially available 2G tapes. Due to its excellent RF and mechanical properties, Kapton became the material of choice for flexible silicone electronics. We show that YBCO-on-Kapton is a promising technology for cryogenic interconnects, current leads, passive RF devices and semiconductor-superconductor hybrids.

II. Experiment

We used a standard 12 mm wide 2G tape supplied by SuperPower Inc [9]. The YBCO layer was attached to 5 mil (125 μm)

Manuscript received ; accepted . Date of publication; date of current version . This work was supported by the Brookhaven National Laboratory under award LDRD #20-023 CC/CSI. *(Corresponding author: Vyacheslav Solovyov.)*

V. F. Solovyov is with Brookhaven Technology Group, 1000 Innovation Road, Stony Brook, NY 11794, (slowa@brookhaventech.com).

Zachary Mendleson is with Brookhaven Technology Group, 1000 Innovation Road, Stony Brook, NY 11794, (zachmendleson@gmail.com)

Olli-Pentti Saira and Ilya Drozdov are with Brookhaven National Laboratory, Upton, NY 11973 (e-mail: osaira@bnl.gov and drozdov@bnl.gov)

Color versions of one or more of the figures in this paper are available online at http://ieeexplore.ieee.org.

Digital Object Identifier

thick Kapton tape (DuPont Corp.) with a cryogenic adhesive. The structure was subjected to a thermal shock as previously described, after which the YBCO layer cleanly separated from the substrate. Fig.1a is a photograph of a 12 mm wide YBCO layer cast onto a 1" (24.5 mm) wide Kapton tape. The signal line structure was patterned by a fiber laser (SPI 70w model) equipped with IntelliScan 14 scan-head. In this arrangement the scan-head processing field was 14x14 cm, which limited the device length to 14 cm. The patterning regime was carefully optimized to ensure removal of the unwanted YBCO material while minimizing thermal stress on the Kapton substrate. Managing thermal stress was essential for the device integrity. The YBCO layer was found to be very prone to cracking due to local overheating of the Kapton support by the laser beam or a soldering iron. Inset in Fig. 1b shows propagation of crack though a signal line due to overheating by the laser beam. The superconducting transition temperature of YBCO film before and after the exfoliation was determined by a mutual inductance method, which measures amplitude of screening currents in a 10x10 mm film sample. The room temperature resistance of an exfoliated film was 33 ± 4 Ω. For a 12 mm wide, 12 cm long, which corresponds to the normal state resistivity of 280 ± 30 μΩ cm and is consistent with the literature data for optimally doped YBCO.

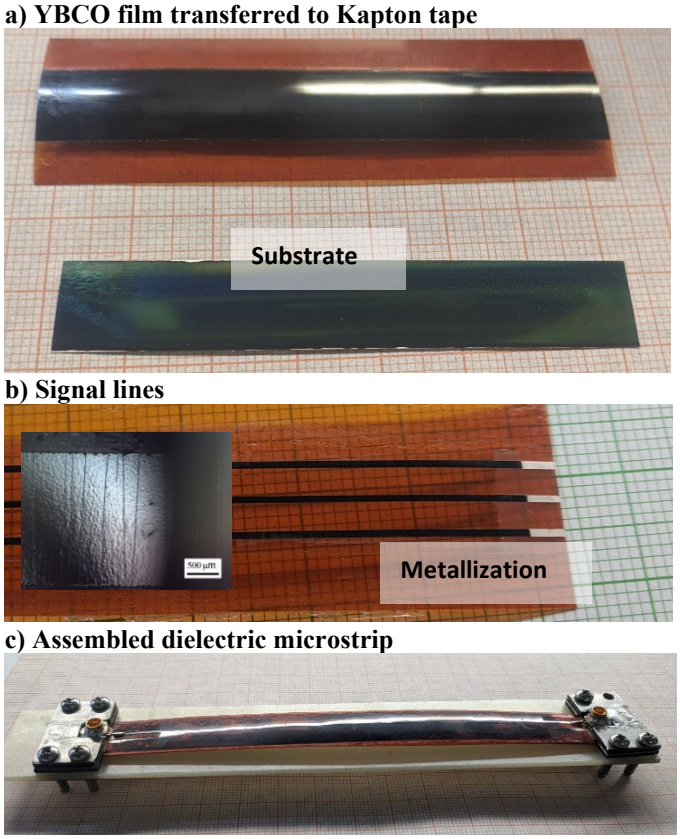

Fig. 1. a) 12 mm wide YBCO film after transfer onto a 5 mil Kapton tape. The metal substrate is on the bottom. b) 0.8 mm wide signal lines patterned by the pulsed fiber laser. Silver metallization pads are visible on the right. The inset in panel b) shows cracking of a signal line due to an excessive laser power level applied during the patterning step c) Assembled 14 cm long dielectric microstrip with a right-angle SMP launch.

After the patterning step the line resistance increased proportionally, to 500 ± 50 Ω. The microstrip robustness was tested by recording the signal and ground plane resistance after immersion of the device into liquid Nitrogen. Both signal and ground plane lines registered < 1 Ω at 77 K after more than 10 thermal cycles between room temperature and 77 K. The films did not show any signs of deterioration when bent down to a 20 mm radius. When the bending tolerance was exceeded by bending to radii smaller than 20 mm , multiple cracks, similar to ones shown in the inset Fig. 1b, developed in the YBCO layer.

Fig. 1b shows an array of 0.8 mm wide signal lines, 3 mm apart, patterened by the pulsed laser method. The silver metallization pads are visible on the right. In the dielectric microstrip structure an un-patterned 12 mm wide film served as the ground plane. The signal line array, shown in Fig. 1b, was glued on top of the ground plane with a cryogenic epoxy. Only one line was used in the experiment, the rest were reserved for the future study of line crosstalk. The signal line width and the dielectric thickness were matched to deliver a 50 Ω impedance of the microstrip. Additionally, a dielectric resonator comprised of a straight 50 Ω line and two excitation (feed) lines with capacitive coupling also was manufactured following the same procedure.

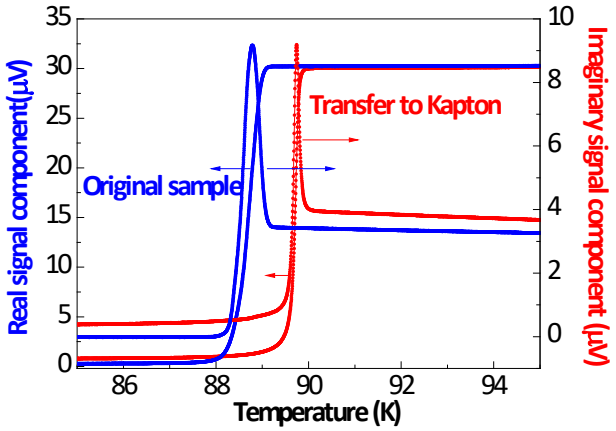

Fig. 2. Superconducting transition detected by the mutual inductance method at 1 KHz. Both real and imaginary part of the signal are shown for the as-received sample (on the metal substrate) and after the YBCO film transferred onto a 5 mil Kapton tape..

Fig.1c presents the assembled dielectric microstrip. The microstrip was terminated with a surface-mounted 50 Ω SMP connector (Molex 0853050232). The conduction cooling test was carried out in a custom vacuum chamber in 2×10^{-6} Torr vacuum, the base tempertaure18 K. The microstrip SMP terminations were thermally anchored to a cold plate of a single stage cryopump (CryoMech model AL230). Both DC resistance measurement and RF insertion loss were performed during the same cooldown. The insertion loss in the conduction cooled regime was measured up to 500 MHz using an Agilent 4395A network analyzer. Measurement up to 6 GHz was performed only at 77 K using a Rohde & Schwarz ZNB series network analyzer.

III. Results

Fig. 2 compares inductive response of the YBCO layer before and after the transfer to Kapton film. The observed T_c enhancement, from 88.8 K to 89.7 K is most likely due to in-plane compression of the YBCO layer upon cool down. YBCO films are grown on substrates with closely matching coefficient of thermal expansion (CTE). YBCO layer contracts by – 0.21% on cooldown from room temperature to 77 K, which is close to that of Hastelloy, – 0.22%. A YBCO film attached to a thicker Kapton tape would experience in-plane compression – 0.25%. Pahlke *et al*. [10] estimates that in-plane compression would enhance T_c by 0.75 K per – 1% of applied compressive strain. The observed T_c enhancement is close to 0.9 K, which is an indication of an in-plane compression level higher than what can be accounted to the Kapton tape alone. It is possible that the epoxy adhesive used to attach the YBCO layer to the Kapton surface exhorts an additional compression.

Fig. 3a is a time profile of DC resistance of the signal line and ground plane during cool-down in the conduction-cooling setup. The systems reached the base temperature, 18 K, after approximately 3 hrs. of operation. The microstrip, which was cooled by conduction through the SMP connectors and radiation, reached the superconducting state after 9 hrs. This is expected considering the exceptionally low thermal conductivity, < 1 $Wm^{-1}K^{-1}$ of the assembly. Frequency dependence of the insertion loss, S_{21}, recorded during the cooldown in 30 min intervals, is presented in Fig. 3b. After the microstrip reached the superconducting state the S_{21} loss was registering below – 0.5 dB, which is within the calibration error for a "short" calibration standard used in the study.

Fig. 3c presents insertion loss spectrum up to 6 GHz in LN2 immersion (77 K). The solid line models the oscillatory features in Fig. 3c as standing waves caused by a parasitic 2 nH inductance at each end of the line. The model does reproduce the overall features of the spectrum suggesting that the line terminations are less than optimally designed. Sharp peaks with ≈ 1 GHz period are resonances in the neighboring unterminated lines, which are positioned 3 mm apart as shown in Fig1b.

The vast majority of today's superconducting quantum hardware operates in the microwave C-band (4 – 8 GHz). We characterize the losses of our test cables in this frequency range in two ways. First, picking the maximum of the S_{21} oscillations and corresponding to constructive interference that cancels the local discontinuity caused by the connectors. We observe approximately 0.5 dB of total insertion loss up to 6 GHz. Second, we estimate the attenuation constant by analyzing the weak resonance features from the neighboring unterminated lines. The losses in k^{th} mode of a λ/2 transmission line resonator are related to the attenuation constant α via:

$$\alpha\ [\mathrm{dB/m}] = 8.68\, k\pi/(2lQ_i) \qquad (1)$$

where l is the physical length of the resonator and Q_i is the internal (unloaded) quality factor. We fitted a standard parallel shunt resonator model to modes 2 through 6. The corresponding attenuation constants are between 0.5 and 1.0 dB/m, for the frequency range from 1.9 GHz to 5.8 GHz spanned by these modes. The visibility of the fundamental mode in the data is too poor to reliably estimate the Q factor.

a) DC resistance during the cooldown

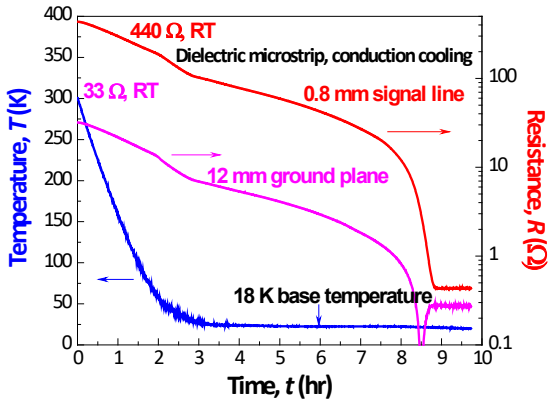

b) Insertion loss evolution during the cooldown

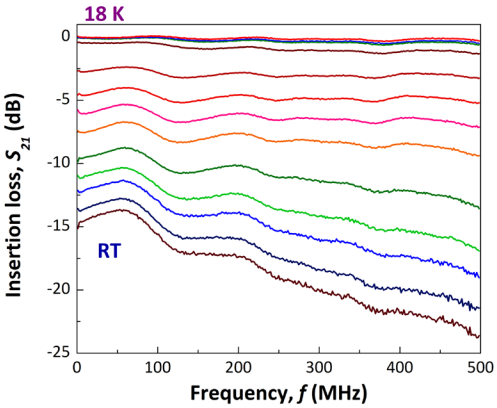

c) Insertion loss up to 6 GHz, 77 K

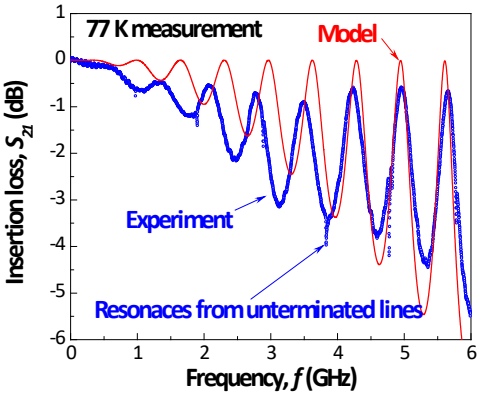

Fig. 3. a) DC resistance of the ground plane and the signal line during the cool down. b) Insertion loss up to 500 MHz during the cooldown in the conduction cooled system. c) Insertion loss up to 6 GHz measured in liquid Nitrogen (77 K) measured at Brookhaven National Laboratory. Sharp features on the spectrum are resonances from unterminated neighboring lines, see Fig. 1b. The solid line is the best fit of the impedance mismatch model, assuming 2 nH parasitic

Fig. 4 shows a spectrum of the first (641 MHz) and second (1.302 GHz) harmonics of a separate, dedicated resonator sample. The resonant frequency is consistent with a simple estimate for a half-wave resonator comprised of a 13 cm long line on a

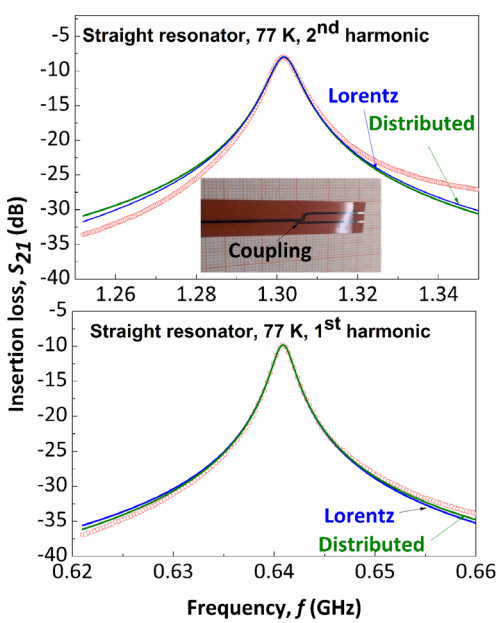

Fig. 4. The resonant curve of the first harmonic (bottom panel) at 0.641 GHz and the second at 1.302 GHz (top panel). The solid lines are the two alternative best-fit models. The Lorentzian model yields a Q-factor of 313 ± 5 for the first harmonic, which we ascribe to coupling losses. The distributed resonance model reproduces the data with a 0.24 pF coupling capacitance. The inset in the upper panel shows the coupling region of the straight dielectric resonator.

Kapton substrate with $\varepsilon = 3.2$. The solid lines are the Lorentzian fit and a fitted transmission line model that has equal coupling capacitors at each end of the resonator, and no internal losses. Both models equally explain the experiment. Due to the lack of an accurate pass-through reference, we cannot distinguish between internal and coupling losses in a single mode. However, noting that the transmission line model indicates similar coupling capacitors for both modes (0.25 pF and 0.23 pF for the first and second harmonics, respectively), it's likely that total Q was dominated by the coupling, and that the internal losses are smaller. Q factors determined from the Lorentzian fit are 312.6 ± 5 for the first harmonic 181.9 ± 0.5 for the second.

IV. Discussion

Excellent RF properties of high-quality HTS films [11, 12] has been demonstrated almost immediately after discovery of HTS. However, high quality films could only be grown on expensive single-crystal substrates. It was shown that even though YBCO layers manufactured by the 2G process lack the structural quality of high-end YBCO films grown on R-cut sapphire, the surface resistance is only marginally higher [13]. Which implied that in YBCO layers grown by large-scale deposition could be suitable for RF applications. Our resonance and transmission data, Fig. 3 and 4, confirm that YBCO grown by a 2G process retains excellent superconducting properties after transfer to Kapton.

We recognize that a simple microstrip geometry tested in this study would be poorly suited as a transmission cable, because a cable comprised of microstrips would exhibit poor isolation between neighboring lines. For example, Walter et al. [14]

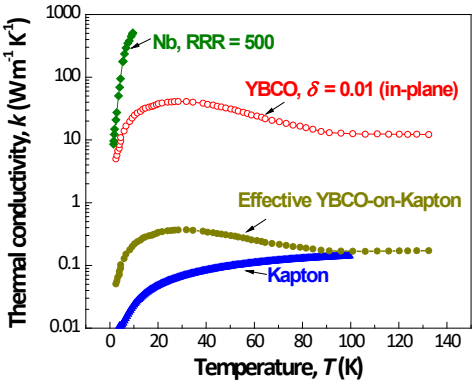

Fig. 5. Thermal conductivity of Kapton and in-plane thermal conductivity of a high-quality YBCO single crystal, adapted from [15]. Thermal conductivity of Nb with RRR = 500 is show for the reference.

measured inter-line isolation, $S_{41} = -25$dB for a Nb-Ti microstrip with a geometry similar to one shown in Fig. 1, which is significantly worse than commonly accepted target – 60 dB. A fully shielded, stripline geometry is more preferable. However, dense rows of grounded vias, or via fences, are essential for suppressing parasitic resonances of the ground plane [15]. A via technology would involve metallization of YBCO ground planes and a method for drilling through the stack. Our preliminary results indicate that this can be accomplished by a combination of laser processing tools.

Finally, we used published thermal conductivity, k, data, Fig. 5, to estimate passive thermal loss of a hypothetical high-density YBCO cable. Because thermal conductivity of YBCO films is not available, we use in-plane thermal conductivity data for a high quality, optimally doped YBCO single crystal [16] as "the worst case" (the highest thermal conductivity) scenario. Unlike low-temperature, s-wave, superconductors, superconductivity in HTS is believed to be of d-wave type. The d-wave symmetry of HTS order parameter leads to nodes in the gap structure and is associated quasiparticle excitations. The characteristic peak in in-plane thermal conductivity of YBCO single crystals is explained by increased mean free path of quasiparticles with cooling [17]. Due to this effect the projected aggregate thermal conductivity of 1μm YBCO on 100 μm Kapton composite, shown in Fig. 5, is still dominated by heat transport through the YBCO layer. Finite element analysis under the "worst case scenario" estimates conduction heat loss at 12 Wm^{-2} for a 1 m long cable between 50 and 4 K, which translates into < 1 μW per line, assuming 1 mm line pitch. This level of heat load can be easily managed by a compact pulsed-tube cooler even for $10^5 - 10^6$ lines computer.

V. Conclusion

In conclusion we demonstrate a feasibility of manufacturing cryogenic devices based on YBCO-on-Kapton technology. The future work will focus on scaling-up the technology to 1 m long high-density flex cables with < 60 dB of crosstalk. This would require development of a reliable and scalable via technology.

REFERENCES

[1] A. M. Kadin, R. J. Webber, and D. Gupta, "Current Leads and Optimized Thermal Packaging for Superconducting Systems on Multistage Cryocoolers," *IEEE Transactions on Applied Superconductivity,* vol. 17, pp. 975-978, 2007.

[2] S. Krinner, S. Storz, P. Kurpiers, P. Magnard, J. Heinsoo, R. Keller*, et al.*, "Engineering cryogenic setups for 100-qubit scale superconducting circuit systems," *EPJ Quantum Technology,* vol. 6, p. 2, 2019/05/28 2019.

[3] A. Kushino and S. Kasai, "Development of Semi-Rigid Superconducting Coaxial Cables as Low-Pass Filters," *IEEE Transactions on Applied Superconductivity,* vol. 27, p. 4, Jun 2017.

[4] J. P. Smith, B. A. Mazin, A. B. Walter, M. Daal, I. J. I. Bailey, C. Bockstiegel*, et al.*, "Flexible Coaxial Ribbon Cable for High-Density Superconducting Microwave Device Arrays," *IEEE Transactions on Applied Superconductivity,* vol. 31, pp. 1-5, 2021.

[5] M. Daal, N. Zobrist, N. Kellaris, B. Sadoulet, and M. Robertson, "Properties of selected structural and flat flexible cabling materials for low temperature applications," *Cryogenics,* vol. 98, pp. 47-59, Mar 2019.

[6] D. B. Tuckerman, M. C. Hamilton, D. J. Reilly, R. Bai, G. A. Hernandez, J. M. Hornibrook*, et al.*, "Flexible superconducting Nb transmission lines on thin film polyimide for quantum computing applications," *Superconductor Science and Technology,* vol. 29, p. 084007, 2016/07/11 2016.

[7] D. Larbalestier, A. Gurevich, D. M. Feldmann, and A. Polyanskii, "High-T-c superconducting materials for electric power applications," *Nature,* vol. 414, pp. 368-377, Nov 15 2001.

[8] V. Solovyov and P. Farrell, "Exfoliated YBCO filaments for second-generation superconducting cable," *Superconductor Science and Technology,* vol. 30, p. 014006, 2017.

[9] Y. F. Zhang, T. F. Lehner, T. Fukushima, H. Sakamoto, and D. W. Hazelton, "Progress in Production and Performance of Second Generation (2G) HTS Wire for Practical Applications," *IEEE Transactions on Applied Superconductivity,* vol. 24, p. 7500405, Oct 2014.

[10] P. Pahlke, S. Trommler, B. Holzapfel, L. Schultz, and R. Hühne, "Dynamic variation of biaxial strain in optimally doped and underdoped $YBa_2Cu_3O_{7-\delta}$ thin films," *Journal of Applied Physics,* vol. 113, p. 123907, 2013.

[11] A. I. Braginski, "Superconductor Electronics: Status and Outlook," *Journal of Superconductivity and Novel Magnetism,* vol. 32, pp. 23-44, Jan 2019.

[12] C. G. Li, X. Wang, J. Wang, L. Sun, and Y. S. He, "Progress on applications of high temperature superconducting microwave filters," *Superconductor Science & Technology,* vol. 30, p. 14, Jul 2017.

[13] W. Jarek, K. Jerzy, Q. Kuang, K. Dhivya, G. Eduard, and S. Venkat, "Microwave characterization of normal and superconducting states of MOCVD made YBCO tapes," *Superconductor Science and Technology,* vol. 30, p. 035009, 2017.

[14] A. B. Walter, C. Bockstiegel, B. A. Mazin, and M. Daal, "Laminated NbTi-on-Kapton Microstrip Cables for Flexible Sub-Kelvin RF Electronics," *IEEE Transactions on Applied Superconductivity,* vol. 28, p. 5, Jan 2018.

[15] G. E. Ponchak, E. M. Tentzeris, and J. Papapolymerou, "Coupling between microstrip lines embedded in polyimide layers for 3D-MMICs on Si," *IEE Proceedings - Microwaves, Antennas and Propagation,* vol. 150, p. 344, 2003.

[16] M. Sutherland, D. G. Hawthorn, R. W. Hill, F. Ronning, S. Wakimoto, H. Zhang*, et al.*, "Thermal conductivity across the phase diagram of cuprates: Low-energy quasiparticles and doping dependence of the superconducting gap," *Physical Review B,* vol. 67, p. 174520, 05/23/ 2003.

[17] P. J. Hirschfeld and W. O. Putikka, "Theory of Thermal Conductivity in $Y_1Ba_2Cu_3O_{7-d}$," *Physical Review Letters,* vol. 77, pp. 3909-3912, 10/28/ 1996.